



Chemically treated *Acacia nilotica* filler-reinforced epoxy composites: tribological studies and optimization of process parameters

D. Jafrey Daniel James¹ · G. Karthik Pandiyan² · Raghunathan Vijay³ · Ayyappan Vinod³ · Mavinkere Rangappa Sanjay³ · Siengchin Suchart³

Received: 29 February 2024 / Accepted: 7 July 2024 / Published online: 15 July 2024
© The Author(s), under exclusive licence to the Institute of Chemistry, Slovak Academy of Sciences 2024

Abstract

The current trend is the ecological consciousness of replacing synthetic fibers with natural fiber. However, several restrictions exist on using natural fibers/fillers, including compatibility, hydrophobicity, and locality. The natural material chosen for the present investigation, *Acacia nilotica*, is short and cylindrical; the same has been used as reinforcement after being chemically treated with silane and grinded into fillers in the present study. Grinded silane-treated *A. nilotica* fillers were added in a range of 0, 2, 4, and 6 weight percent to the epoxy matrix. Conventional hand layup was used to manufacture composite materials using epoxy resin and hardener. The manufactured composite's tribological properties were evaluated according to ASTM G99-17 using the pin-on-disk machine under two-body abrasive wear conditions. L-16 orthogonal arrays were used to conduct the research. Load, sliding distance, and material were the process input parameters, and the results were evaluated using the Specific Wear Rate (SWR) and Coefficient of Friction (COF). Analysis of variance (ANOVA) was used to analyze the significant variables. EDAS was used to optimize the output. The abraded surfaces were finally studied using worn surface morphology. According to the findings, silane-treated *A. nilotica* filler is a new and promising resource as a sustainable raw material for reinforcement in polymer composites manufacturing lightweight materials. Results revealed that the optimized values were 6 wt%, load at 20 N, and sliding distance of 225 m. SWR values decreased by 61.2%, and COF values decreased by 34.3% in the case of 6 wt% composites compared to the unreinforced fiber composites. The rank of the sample was assigned according to performance by the EDAS process.

Keywords *Acacia nilotica* · Chemical treatment · ANOVA · Abrasive wear · Load

Introduction

Natural fiber/fillers, a renewable resource, have unique qualities that are important for eco-friendly composites (Yahiya and Venu 2022; Singh et al. 2023). Various natural fibers/

fillers such as banana, hemp, and wood fillers were used as potential reinforcement sources in composite fabrications (Vijay et al. 2022). The development of natural fiber components in established composites was helped by the abundance of natural fibers (Raghunathan et al. 2022; Vinod et al. 2023). As a result, they have more benefits than synthetic fiber; for instance, they are biodegradable, cheap, less dense, and have enhanced durability (Ramesh et al. 2022). Natural fibers have numerous advantages compared to synthetic fibers, such as abundant availability, cost efficiency, low weight, ease of processing, and environmental friendliness. The natural fiber/fillers were subjected to various chemical treatments to maximize their potential benefits. Researchers in the past chemically treated natural fibers/fillers with different chemicals and reported improvement in various properties (Bhagyashekar and Rao 2007; Reddy et al. 2020; Madhu et al. 2020).

✉ Mavinkere Rangappa Sanjay
mccemrs@gmail.com

¹ Department of Mechanical Engineering, K. Ramakrishnan College of Engineering, Tiruchirappalli, Tamil Nadu, India

² Department of Mechanical Engineering, Sri Vidya College of Engineering and Technology, Virudhunagar, Tamil Nadu, India

³ Natural Composites Research Group Lab, Department of Materials and Production Engineering, The Sirindhorn International Thai-German Graduate School of Engineering (TGGS), King Mongkut's University of Technology North Bangkok (KMUTNB), Bangkok, Thailand

Epoxy resin is a popular polymer matrix due to its strong adhesion when fibers/fillers are added. Epoxy material is an excellent option due to its increased hardness, humidity resistance, superior hardness qualities, and improved thermal and mechanical properties. Fillers are frequently used to increase the characteristics of the epoxy matrix (Ramesh et al. 2022). Researchers recently incorporated particles and short fibers as fillers into the epoxy matrix. Some parameters that influenced output characteristics include the shape of the fillers, the amount of filler applied, and the treatment of the reinforcement. Surface-modified fillers, among other things, can improve wear, dimensional stability, and heat dissipation (Bhagyashekar and Rao 2007).

Recent studies reinforced the epoxy matrix with *Setaria italic* fiber that was 10% alkali-treated. Comparing treated and untreated fiber-reinforced composites, alkali treatment increased tensile (35.1%) and flexural strength (8.6%) (Reddy et al. 2020). Madhu et al. (2020) chemically modified *Prosopis juliflora* fiber with various chemical treatments like sodium hydroxide, stearic acid, and peroxide treatment. They found an increase in the properties of the chemically treated fibers compared to the untreated fibers, chemically treated with acetylene and alkaline solutions. The hand layup process was used to manufacture the composites. The main intention was to study dynamic mechanical analysis, strength, impact, and hardness of the manufactured fibers. When compared to acetylene-treated fiber samples, alkaline-treated natural fiber samples had the best strength, impact, and hardness characteristics, mainly due to the strong bonding between matrix and fiber (Kumar et al. 2023). Silane treatment was the most used treatment of natural fibers in this study as it enhances compatibility between the matrix, ensures better thermal stability, increases composite strength, reduces fiber alkalinity, and increases composite performance. It solves moisture absorption, reduces fiber degradation, and makes natural fibers the perfect material for many applications.

The tribological properties of any composite are explored to study their friction characteristics. The wear properties of a material depend on its properties. Abrasive wear is the primary cause of wear and a common method for material removal in industry. It eliminates solid particles from another body via complex particle movement (Formisano et al. 2016). Abrasive wear is the result of abrasive particles rubbing against a solid surface. Abrasive wear is caused by two mechanisms: loss of material from the front end of abrasive particles sliding on the surface and the creation of grooves caused by pushing abrasive grit onto the surface (Raghunathan et al. 2021). To increase their properties, epoxy composites are reinforced with varied fillers, both natural and artificial. Numerous researchers attempted to enhance its function by incorporating various fillers and reinforcing agents, including nano-particles. Fillers

are provided pre-treatments to improve interfacial contact between the matrix and filler. These initiatives successfully enhanced the composites' mechanical and tribological characteristics (Albert et al. 2022).

Sudheer et al. (2014) studied their tribological characteristics using alkali-treated *Vachellia farnesiana* fibers at various weight concentrations. It was concluded from their output that an increase in reinforcement resulted in increased wear resistance. Shi et al. (2004) manufactured composite epoxy/PTW composites and studied their tribological and mechanical properties. The addition of PTW increased properties like density and stiffness and decreased ductility. Xing and Li (2004) reinforced nano-aluminum oxide into the epoxy matrix, increasing flexural modulus and strength. In addition, they concluded that they found more wear resistance compared to a pure epoxy matrix. When nano-aluminum oxide was pre-heated, it increased several properties. Durand et al. (1995) employed nano-particles of 500 nm, whereas Nirmal et al. (2010) utilized nano-particles of 100 nm to examine composites' wear rate. Durand's findings implied a positive link between particle size and wear resistance, contrary to the findings of Xing and Li. Due to variations in testing parameters, the results exhibited conflicting outcomes. Durand exerted a force of 10 N, whereas Xing and Li applied a load of 2 N. In 2010, Salisu et al. (2016) used NaOH-treated betel fibers to strengthen a polyester matrix, and untreated ones were subjected to tribological studies. The study demonstrated that treating fiber with a 6% NaOH solution improved wear resistance in composite materials.

The fiber selected for the present study is *Acacia nilotica*, a plant that grows to a height of 20 m with a spherical crown. Its branches are usually made of black and gray-pinkish stems. It has thin gray spines as auxiliary pairs. It has 3 to 12 pairs, each 7.5 cm long. It has a diameter of 3 cm. It is usually grown in drier areas of Africa, Egypt, South Africa, India, and Sri Lanka. It is found on roadsides and agricultural lands in India. It is an isolated tree which is rarely seen in patches. Birniwa et al. (2019) studied the physio-mechanical characteristics of *A. nilotica* fiber, which was treated by alkali, silane, and benzoylation. They concluded that there was an increase in resistance to the absorption of water and an increase in the interaction between the fiber and matrix. Jafrey and Panneerselvam (2017) studied the mechanical characteristics of *Acacia nilotica*/glass fiber/epoxy composites. *Acacia nilotica* was initially treated by peroxide and benzoylation treatment processes. They concluded that the mechanical properties of the composites increased when chemically treated compared to those untreated.

The Taguchi methodology is most commonly used to design experiments, which reduces their complexity. It reduces the number of experiments, and one infers more data from the least number of experiments. Taguchi methodology

is applied to the field of product development. It is used to improve quality, reduce variation, and improve performance. It can also produce efficient results if multiple factors interact. Several researchers, like Kumar et al. (2022), Joseph and Panneerselvam (2021), and Vikram et al. (2020), used Taguchi methodology for the design of experiments. ANOVA methodology is used to find how input factors affect output performance. It is a statistical tool used to compare means in the case of multiple groups and to make conclusions about the dataset being studied.

Optimization is the standard methodology for finding optimized parameters from multiple output parameters. Researchers used various optimization techniques to maximize their output values. The VIKOR technique was applied—in dry and low lubricant conditions—for multi-response optimization during the conventional turning of AISI 316L steel (Pandiyan et al. 2021). Fuse et al. (2021) used response surface methodology to optimize the machining characteristics of AA6061-T6/15 wt% SiC composites. Raghunath et al. (2021) utilized both fuzzy AHP and fuzzy TOPSIS to optimize the EDM machining of Ti6Al4V, with the experiments being designed according to response surface methodology. Kumar et al. (2013) used the ARAS approach to utilize LINGO analysis to optimize the mechanical properties of glass and sisal fiber-reinforced composites. The machinability characteristics of EN 24 steel were optimized by the AHP and VIKOR methodologies by Bahadur (2000).

It can be concluded from the above literature that there were works related to extracting and characterizing natural fibers. A broad literature search revealed no work on manufacturing and reinforcing silane-treated *A. nilotica* fillers in the epoxy matrix. There were also no works related to the tribological characteristics of silane-treated *A. nilotica* fillers in epoxy matrix. The current study commenced by extracting *A. nilotica* fibers from the bark, which were retted manually to produce fiber. The extracted fibers underwent silane chemical treatment. Subsequently, the acquired fibers were pulverized to create fillers. The hand layup technique was employed for the production of composites. The fabricated composites were examined for tribological characterization by two-body abrasive wear. The tests were planned using an orthogonal L-16 array. The VIKOR approach was used to optimize the results. Finally, worn surface morphology was used to study wear mechanisms.

Materials and methods

This section details the material utilized, the manufacturing procedure, and the tribological characterization of the created composites.

Material selected

The investigation's matrix was chosen as LY 556-grade epoxy, which had better chemical resistance, was compatible with all manufacturing processes, and was readily available. In the current investigation, HY 951 was selected as the hardener as it was compatible with LY 556, had better curing properties, and resisted chemicals. The Huntsman Company provided both resin and hardener. The natural fiber selected for the present study was *A. nilotica*, belonging to the family of flowering trees, Fabaceae. Initially, the bark was collected from the tree and soaked in water for 20 days to facilitate the loosening of the fiber bundles. The fibers were subsequently extracted from the loosened barks using hand retting. Subsequently, the fibers were subjected to a seven-day drying process under direct sunlight to eliminate surface moisture. In the current investigation, silane-treated *A. nilotica* fibers were used as reinforcement; 2% 3-glycidoxypropyltrimethoxysilane was mixed with a mixture of distilled water and ethanol in a ratio of 1:1 to obtain the silane solution. A pH of 4 was maintained using a glacial acetic acid solution. Silane-treated *A. nilotica* fibers were prepared with 250g fiber in silane for 2 h. It was dried in a hot air oven at 50 °C for 24 h. Then, silane-treated *A. nilotica* fibers were grinded using a universal milling machine and sieved to 50–70 μm. The chemical composition of silane-treated *A. nilotica* filler is shown in Table 1.

Composites manufacturing

The hand layup method was used to produce the composites. The epoxy matrix was reinforced with four distinct compositions of silane-treated *A. nilotica* filler samples identified as 1, 2, 3, and 4 with weight percentages of 0, 2, 4, and 6 silane-treated *A. nilotica* filler with the remaining resin matrix. A mold release agent was first applied to remove the material from the surface. Polywax was used as a mold release agent in the present study. A

Table 1 Chemical constituents of silane-treated and untreated *Acacia nilotica* filler

| Cellulose filler name | Cellulose (wt%) | Hemicellulose (wt%) | Lignin (wt%) | Wax (wt%) | Moisture content (%) | Ash (wt%) |
|---------------------------------------|-----------------|---------------------|--------------|-----------|----------------------|-----------|
| Silane-treated <i>Acacia nilotica</i> | 51.3 | 5.1 | 3.9 | 1.2 | 5.4 | 8.5 |
| Untreated <i>Acacia nilotica</i> | 47.6 | 6.9 | 4.8 | 2.3 | 7.6 | 9.3 |

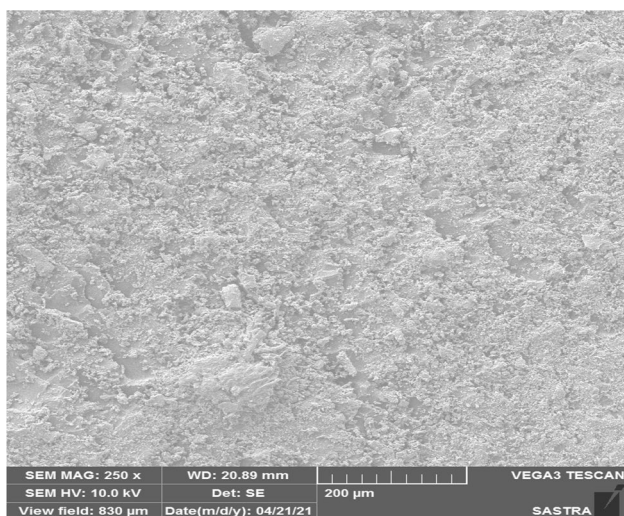


Fig. 1 SEM image of 6 wt% silane-treated *Acacia nilotica* filler-based composite

10:1 ratio between epoxy and hardener was maintained. The epoxy–hardener mixture was then supplemented with reinforcement. After pouring the combined solution into the die material, it cured at room temperature. The wear test samples were cut according to ASTM specifications

using an abrasive water jet cutter (Sudheer et al. 2014). The SEM image of 6 wt% silane-treated *A. nilotica* filler-based composite is shown in Fig. 1. The SEM image noted that there was good interfacial adhesion between the fillers and matrix as a result of silane treatment.

Two-body abrasive wear studies

Using pin-on-disk equipment, friction and wear properties of the manufactured composites were assessed by ASTM G99-05. The line diagram of the tribological setup is shown in Fig. 2. The samples were initially cleaned with acetone, and the uniformity of the contact surface was examined. The steel disk that served as the counter face was covered with 320-grit abrasive paper. The input process parameters for the experiments were material (wt%), load (N), and sliding distance (m). Table 2 shows the input process parameters. A constant 0.5 m/s sliding velocity was set throughout the entire experiment. The studies were conducted using L-16 orthogonal arrays, and the output process parameters evaluated were COF and SWR. COF and SWR are calculated using Eqs. (1 and 2).

Equations: 1 and 2.

Fig. 2 Line diagram of pin-on-disk setup (Formisano et al. 2016)

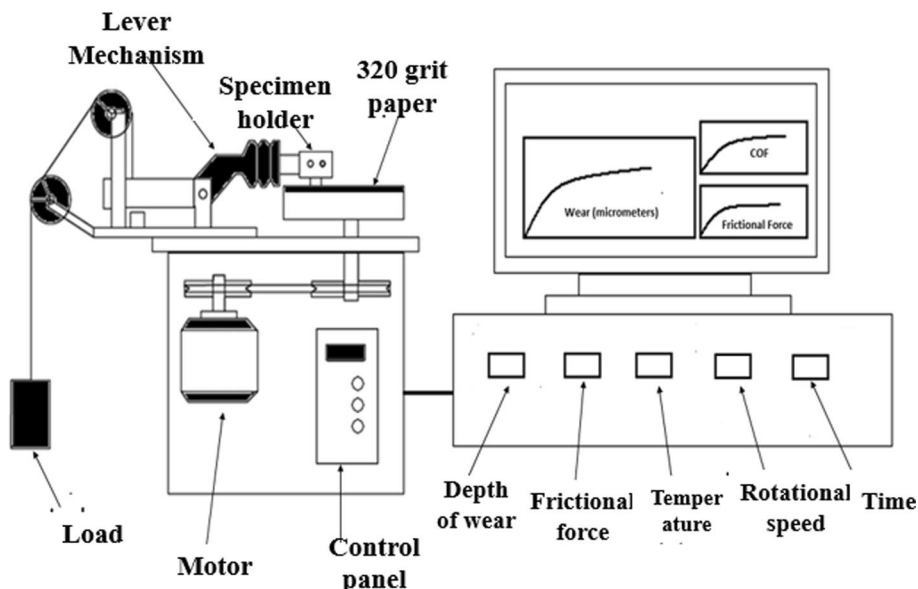


Table 2 Input and output process parameters and their respective levels

| Factor | Process parameter | Unit | Levels | | | |
|--------|-------------------|------|---------|---------|---------|---------|
| | | | Level 1 | Level 2 | Level 3 | Level 4 |
| A | Material | wt% | 0 | 2 | 4 | 6 |
| B | Load | N | 10 | 20 | 30 | 40 |
| C | Sliding Distance | m | 100 | 200 | 300 | 400 |

$$\text{SWR} = \frac{w_1 - w_2}{\rho \times N \times S} \quad (1) \quad \text{COF} = \frac{\text{Frictional Force}(F)}{\text{Applied Load}(N)} \quad (2)$$

where w_1 and w_2 —weight of specimen before and after test, ρ —material density (g/mm^3), N —applied Load (N), and S —sliding distance (m).

Table 3 Input parameters with their output responses for all the experiments

| Sl. no. | Input parameters | | | Output parameters | |
|---------|------------------|----------|----------------------|---|---------------|
| | Material (wt%) | Load (N) | Sliding distance (m) | SWR ($\text{mm}^3/\text{N}\cdot\text{m}$) | COF (μ) |
| 1 | 1 | 5 | 100 | 9.142 | 0.32929 |
| 2 | 1 | 10 | 200 | 8.723 | 0.32266 |
| 3 | 1 | 15 | 300 | 5.836 | 0.29835 |
| 4 | 1 | 20 | 400 | 3.835 | 0.27073 |
| 5 | 2 | 5 | 200 | 8.815 | 0.29617 |
| 6 | 2 | 10 | 100 | 7.500 | 0.28247 |
| 7 | 2 | 15 | 400 | 4.500 | 0.26455 |
| 8 | 2 | 20 | 300 | 3.406 | 0.26245 |
| 9 | 3 | 5 | 300 | 5.491 | 0.24047 |
| 10 | 3 | 10 | 400 | 4.838 | 0.23558 |
| 11 | 3 | 15 | 100 | 5.930 | 0.23362 |
| 12 | 3 | 20 | 200 | 4.543 | 0.24047 |
| 13 | 4 | 5 | 400 | 4.664 | 0.22927 |
| 14 | 4 | 10 | 300 | 3.542 | 0.22267 |
| 15 | 4 | 15 | 200 | 4.145 | 0.22738 |
| 16 | 4 | 20 | 100 | 3.923 | 0.21606 |

Results and discussion

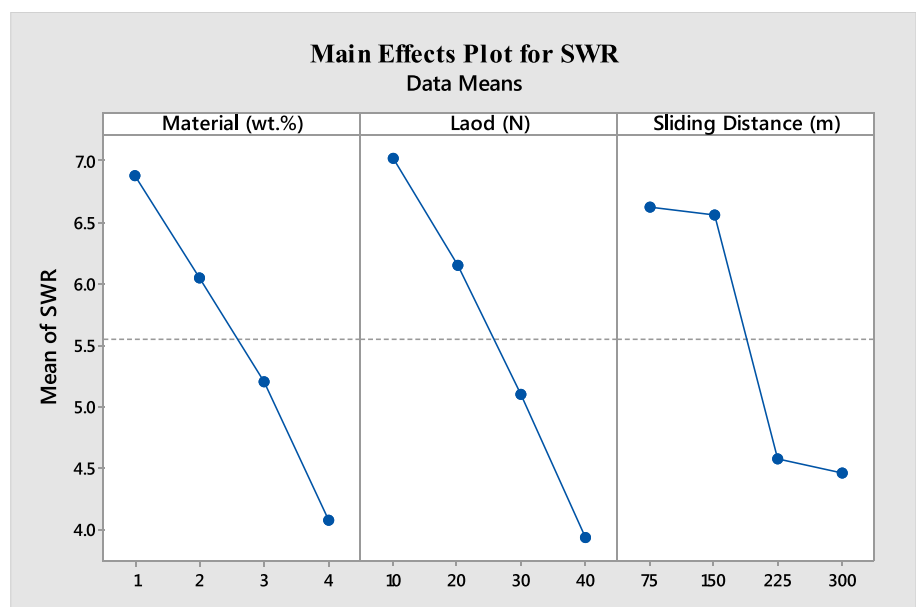
The experiments were planned and carried out according to L-16 orthogonal arrays. The SWR and COF were analyzed, and the results are discussed in the following section. The input and output values are shown in Table 3.

SWR

The main effect plots concerning the SWR for input factors are shown in Fig. 3. The manufactured epoxy composites revealed a high SWR of up to 200 m, and with a further increase in sliding distance, SWR values decreased. When the sliding distance was 400 m, the outer layer became exposed, forming a transfer layer on the abrading surface. When the material slid over the same layer repeatedly, SWR decreased. The transfer layer on the surface served as a lubricating layer to prevent more material from being removed for higher sliding distances. When the sliding distance was set at 100 m, the layer was not exposed fully, which increased SWR values. Thus, the failure to form the transfer layer increased SWR values. A similar trend was also observed by Jafrey and Panneerselvam (2020).

Figure 2 demonstrates a drop in SWR when a load of 40 N was applied, with an increase in SWR values when a load of 10 N was applied. The outer layer was exposed at higher loads, thereby exposing the added filler material. The exposed filler material acted as a thermal insulator, reducing

Fig. 3 Main effect plots of SWR



SWR values. The transfer layer formed was also a reason for SWR reduction at higher load values. When the material was considered, pure material's SWR value was maximum. The main cause of the higher SWR values was the absence of fillers. SWR values decreased due to the addition of filler to the epoxy matrix. SWR values dropped as the amount of fillers in the epoxy matrix increased. Due to their interaction, better bonding between the filler and matrix leads to reduced SWR values. Nirmal et al. (2010) also concluded that there was a decrease in SWR due to an accumulation of fillers in the manufactured composites.

COF

The main effect plots concerning input parameters for output parameters are shown in Fig. 4. Due to the change in the area of contact and the manufactured epoxy composite's strength (shear), there was an increase in friction before reaching a steady state. The epoxy matrix shared the load, and fillers were added to it. The COF was highest for the pure epoxy material (i.e., 0 wt%) and decreased as the percentage of reinforcement increased. The variation of COF concerning the applied load is shown in the figure. It is evident from the figures that the values of COF decreased as the values

of load increased. The decrease in COF values was due to a change in temperature at the contact surface. When the load was set at 40N, heat accumulation was more significant, resulting in the partial melting of the material and the formation of a lubricating surface on the abrasive surface. So, the lubricating surface was a key reason the COF values went down as load values increased.

The values of COF concerning the sliding distance are shown in Fig. 2. There was a quick increase in COF values up to 200 m sliding distance and a decrease after a further rise. The clogging of materials on the wear surface was the reason for decreased COF values at higher sliding distances. Jankovic et al. (2021) also concluded that when sliding distance increased, there was a decrease in COF in the polypropylene composites. A similar observation was also reported by Pandiyan et al. (2022).

ANOVA

The methodology used to determine whether an input process parameter predominates the output process parameter is known as an ANOVA (Bhuyan and Routara 2016). Tables 4 and 5 display the COF and SWR ANOVA results. The fact that the calculated F values were higher than the F table

Fig. 4 Main effect plots of COF

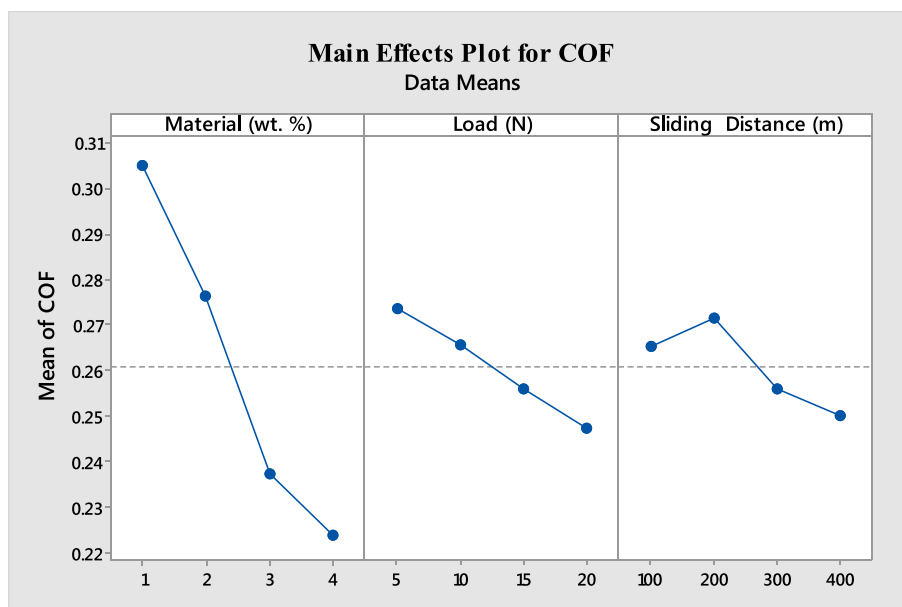
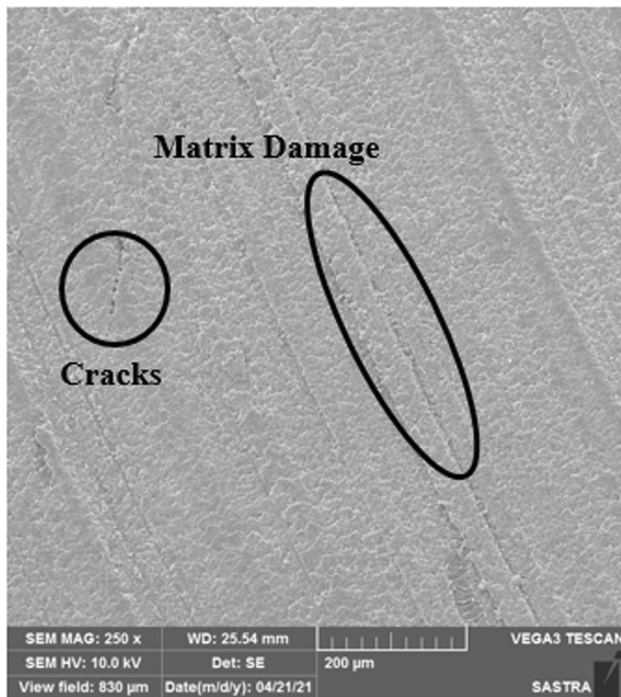


Table 4 ANOVA values of COF

| Source | DOF | Adj. SS | Adj. MS | F_{table} | F_{cal} | % contribution |
|----------------------|-----|----------|----------|-------------|-----------|----------------|
| Material (wt%) | 3 | 0.016508 | 0.005503 | 4.76 | 101.64 | 84.51 |
| Applied load (N) | 3 | 0.001586 | 0.000529 | 4.76 | 9.77 | 8.12 |
| Sliding distance (m) | 3 | 0.001113 | 0.000371 | 4.76 | 6.85 | 5.69 |
| Error | 6 | 0.000325 | 0.000054 | – | | 1.68 |
| Total | 15 | 0.019532 | | | | 100 |

Table 5 ANOVA values of SWR

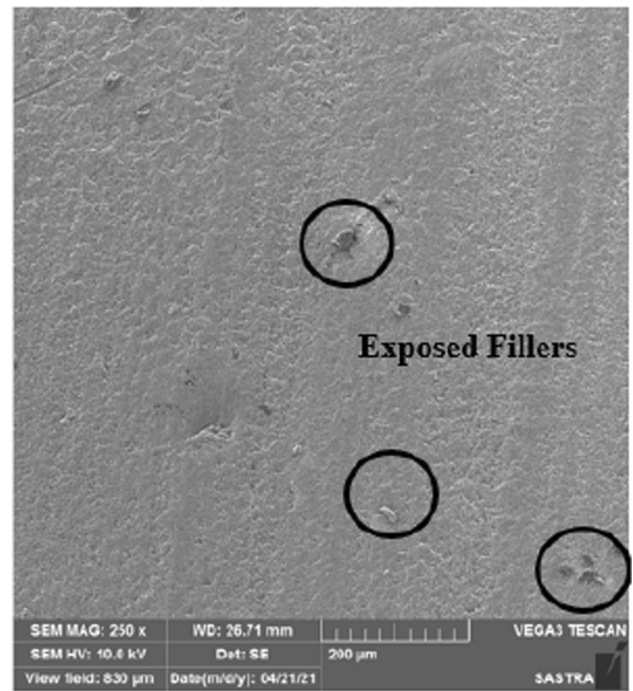
| Source | DOF | Adj. SS | Adj. MS | F_{table} | F_{cal} | % contribution |
|----------------------|-----|---------|---------|-------------|-----------|----------------|
| Material (wt%) | 3 | 17.407 | 5.8024 | 4.76 | 32.85 | 30.39 |
| Applied load (N) | 3 | 21.521 | 7.1738 | 4.76 | 40.61 | 37.58 |
| Sliding Distance (m) | 3 | 17.271 | 5.7570 | 4.76 | 32.59 | 30.16 |
| Error | 6 | 1.060 | 0.1767 | – | – | 1.85 |
| Total | 15 | 57.260 | – | – | – | 100 |

**Fig. 5** Worn surface morphology of pure epoxy composite sample (0 wt% filler)

values in ANOVA demonstrates that all input factors were significant. Tables 4 and 5 reveal that material (84.51%) was the primary factor for COF. By 37.58%, the applied load was the most critical factor in SWR. Sliding distance was the least important factor in both situations.

Worn surface morphology

Worn surface morphology is used to study wear mechanisms on the abraded surface. A scanning electron microscope is used to study the microstructure of the abraded surfaces. Figures 5 and 6 show the SEM images of pure epoxy and 6 wt% silane-treated *A. nilotica* filler-based composite samples. Figure 4 clarifies that, compared to other materials, the

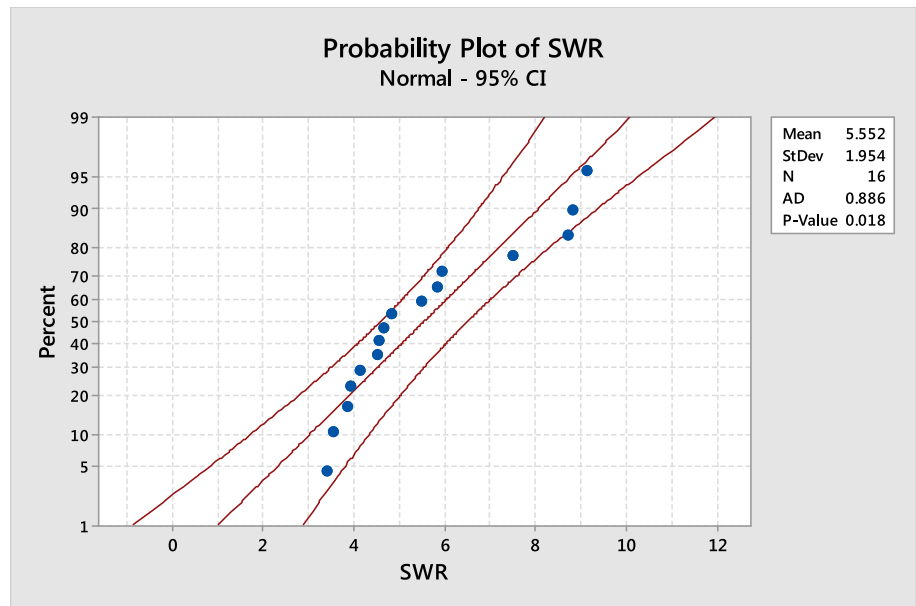
**Fig. 6** Worn surface morphology of 6 wt% silane-treated *Acacia nilotica* filler-based composite

absence of fillers leads to significant wear loss. The image demonstrated how matrix deformation and cracking parallel to the sliding direction emerge. Figure 5 indicates that wear resistance increased with the addition of fillers. The filler acts as a third particle to stop wear from developing, increasing wear resistance. Hence, the worn surface morphology results were similar to the experimental results.

Regression equation

The polynomial equation was developed to analyze the output response using statistics. The minus and plus signs denote the external and internal influences on output quality. The R-sq. values of SWR and COF were 98.15% and

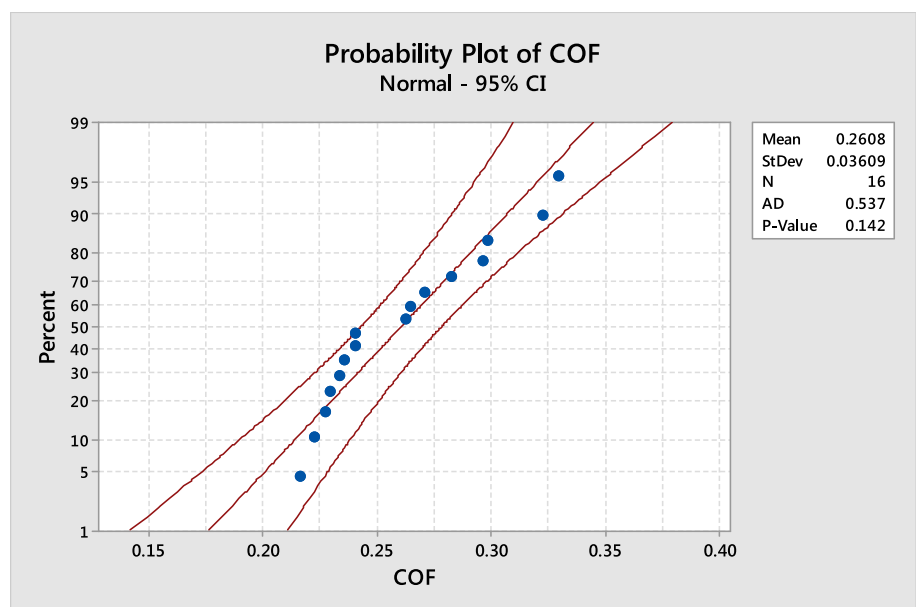
Fig. 7 Residual plots for MRR



98.34%, respectively. The regression equation for SWR and COF is shown in Eqs. (3 and 4).

$$\begin{aligned}
 \text{SWR} = & 5.552 + 1.332 \text{ Material(wt\%)}_1 + 0.503 \text{ Material(wt\%)}_2 \\
 & - 0.352 \text{ Material(wt\%)}_3 - 1.484 \text{ Material(wt\%)}_4 \\
 & + 1.476 \text{ Load (N)}_{10} + 0.599 \text{ Load(N)}_{20} - 0.450 \text{ Load (N)}_{30} \\
 & - 1.625 \text{ Load(N)}_{40} + 1.071 \text{ Sliding Distance(m)}_{75} \\
 & + 1.004 \text{ Sliding Distance (m)}_{150} - 0.983 \text{ Sliding Distance(m)}_{225} \\
 & - 1.093 \text{ Sliding Distance(m)}_{300}
 \end{aligned} \tag{3}$$

Fig. 8 Residual plots for COF



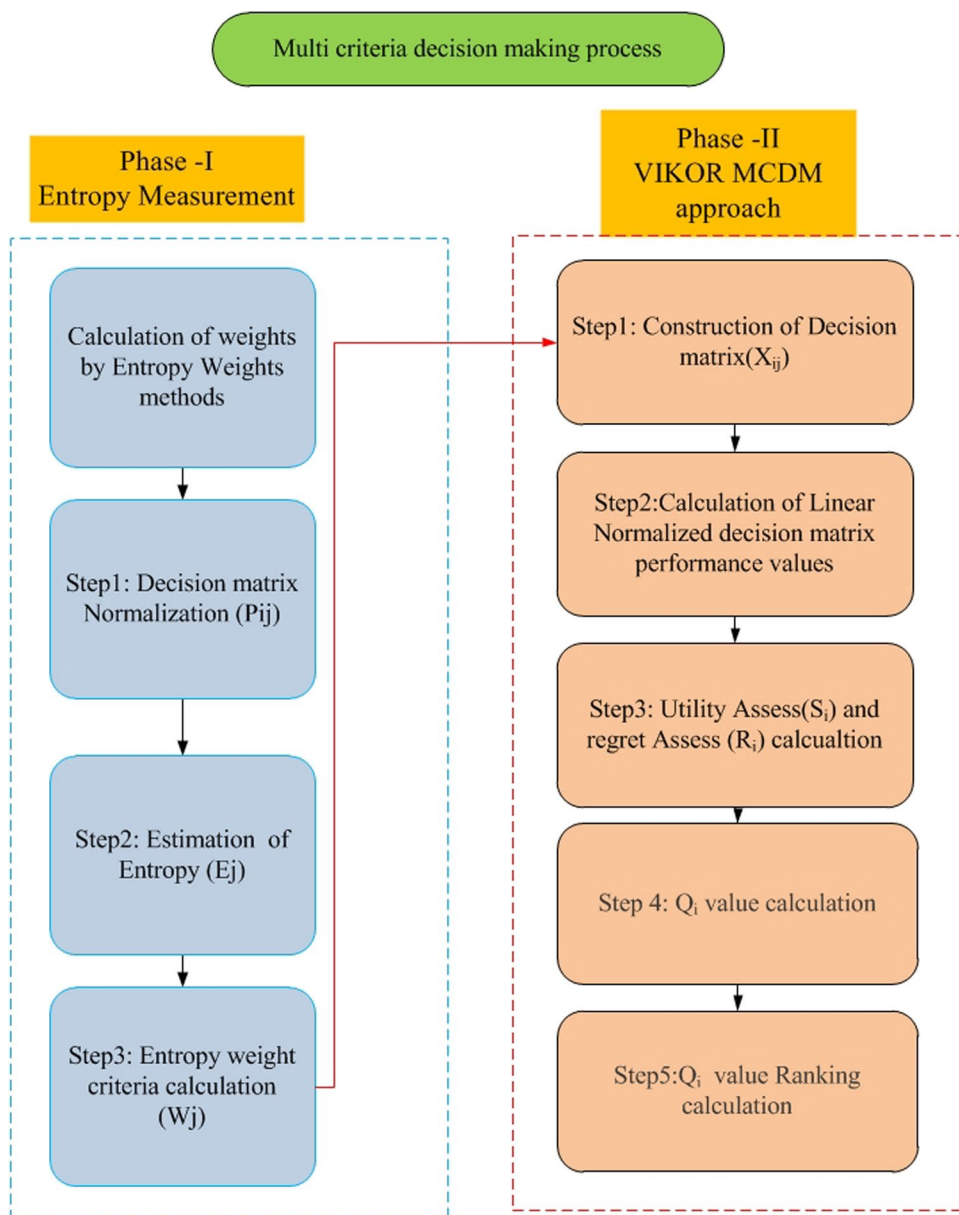
$$\begin{aligned}
 \text{COF} = & 0.26076 + 0.04449 \text{ Material(wt\%)}_1 + 0.01565 \text{ Material(wt\%)}_2 \\
 & - 0.02323 \text{ Material(wt\%)}_3 - 0.03692 \text{ Material(wt\%)}_4 \\
 & + 0.01304 \text{ Load(N)}_{10} + 0.00508 \text{ Load (N)}_{20} \\
 & - 0.00478 \text{ Load (N)}_{30} - 0.01334 \text{ Load(N)}_{40} \\
 & + 0.00460 \text{ Sliding Distance (m)}_{75} + 0.01091 \text{ Sliding Distance(m)}_{150} \\
 & - 0.00478 \text{ Sliding Distance(m)}_{225} - 0.01073 \text{ Sliding Distance (m)}_{300}
 \end{aligned}
 \tag{4}$$

Residual plots

The residual plots for SR and MRR are shown in Figs. 7 and 8. The 45° single-direction observations in these figures show a typical probability contribution and decline, as shown by the systematic possibility graphs. According to Fit

vs. residual plots, the predictable output values of residuals fit the experimental data with no error. SWR and COF standard residual distributions are depicted in the histogram. Figures 6 and 7 reveal that all the points fall within a straight line, indicating normally distributed data.

Fig. 9 Schematic of the optimization process



Determination of weights criteria by Entropy

The mathematical assumption used to establish weights for MCDM problems was put forth by C.E. Shannon in 1948. By rating the alternatives according to their performance traits, the MCDM-based technique evaluates ideal process parameters. The weights determined by entropy techniques were defined using the following processes. A schematic of the optimization process is shown in Fig. 9.

Step 1: Decision matrix normalization (P_{ij})

: The normal decision matrix is calculated by Eq. (5).

$$P_{ij} = \frac{x_{ij}}{\sum_{i=1}^m x_{ij}} \quad (5)$$

($i \in \{1, 2, \dots, n\}$, ($j \in \{1, 2, \dots, m\}$)); where X_{ij} —of i th attribute on j th criterion performance value.

Step 2: Estimation of entropy:

Equation 6 is utilized for the calculation of entropy.

$$E_j = -K \sum_{i=1}^m p_{ij} \ln p_{ij} \quad (6)$$

where $k = 1 / \ln(m)$.

Step 3: Entropy weight criteria calculation (W_j):

$$W_j = \frac{1 - E_j}{\sum_{j=1}^n (1 - E_j)} \quad (7)$$

where W_j —weights criteria.

The above equations calculated weights as 0.861 for SWR and 0.138 for COF.

VIKOR methodology

The following steps are followed for the VIKOR methodology

aaa:

Step 1. Construction of decision matrix (x_{ij}):

$$X = [x_{ij}]_{n \times m} = \begin{bmatrix} x_{11} & x_{12} & \dots & x_{1m} \\ x_{21} & x_{22} & \dots & x_{2m} \\ \vdots & \vdots & \vdots & \vdots \\ x_{n1} & x_{n2} & \dots & x_{nm} \end{bmatrix} \quad (8)$$

where X_{ij} ($X_{ij} \geq 0$), ($i \in \{1, 2, \dots, n\}$) and ($j \in \{1, 2, \dots, m\}$) indicates the performance value of i th attribute on j th decisive factor.

Step 2. Calculation of linear normalized decision matrix performance values:

$$f_{ij} = \frac{f_i^j}{\sqrt{\sum_{i=1}^m (f_i^j)^2}} \quad I = 1, 2, \dots, m, \quad j = 1, 2, \dots, n \quad (9)$$

Step 3. Utility assess (S_j) and regret assess (R_j) calculation:

$$S_j = \sum_{i=1}^n w_i (f_i^* - f_{ij}) / (f_i^* - f_i^-) \quad \text{For Beneficial Attributes} \quad (10)$$

$$S_j = \sum_{i=1}^n w_i (f_i^* - f_{ij}) / (f_i^* - f_i^-) \quad \text{for non-beneficial attributes} \quad (11)$$

$$R_j = \max_i [w_i (f_i^* - f_{ij}) / (f_i^* - f_i^-)] \quad \text{for beneficial attributes} \quad (12)$$

$$R_j = \max_i [w_i (f_i^* - f_{ij}) / (f_i^* - f_i^-)] \quad \text{for non-beneficial attributes} \quad (13)$$

Step 4. Q_i value calculation:

$$Q_j = V * \frac{(S_j - S^*)}{S^- - S^*} + (1 - v) \frac{(R_j - R^*)}{R^- - R^*} \quad (14)$$

(V values lie between 0 to 1, as we take 0.5)

Step 5. Q_i value ranking calculation

: Table 6 shows that experiment number 14 had the greatest appraisal score of 0.988, which was nearer 1. The VIKOR score revealed that the input parameters, like material, were 6 wt%, load at 20 N, and sliding distance of 225 m and they yielded better characteristics. Based on the evaluation, the options were sorted according to the appraisal score values as $14 < 8 < 16 < 4 < 15 < 12 < 7 < 2 < 10 < 9 < 11 < 3 < 6 < 5 < 2 < 1$.

Conclusions

The *A. nilotica* fibers were initially collected from the bark and transformed into fibers through manual retting. It was then treated with silane, dried, and crushed into the filler. Composites containing 0, 2, 4, and 6 wt% silane-treated *A. nilotica* filler-based epoxy composites were produced through hand layup. The tribological performance was studied by the two-body abrasive wear process using L-16 orthogonal arrays with input process parameters like material, load, and sliding distance. Outputs evaluated were SWR and COF. The experimental results showed that adding 6 wt% filler, 10N load, and 400 m sliding distance increased wear resistance. SWR values decreased by 61.2%, and COF values decreased by 34.3% in the case of 6 wt% composites

Table 6 Optimization of output values by VIKOR method

| Sl. no. | Input parameters | | | Output with weights | | | | Normalized decision matrix | | Utility access | | Regret analysis | | Appraisal score | Rank |
|---------|------------------|------|------------------|---------------------|-----------|-------------|--------|----------------------------|----------|----------------|----------------|-----------------|----------|-----------------|------|
| | Material | Load | Sliding distance | SWR (0.861) | | COF (0.138) | | SWR | COF | S _i | R _i | Q _i | | | |
| | | | | SWR | COF | SWR | COF | | | | | | | | |
| 1 | 1 | 5 | 100 | 9.1416 | 0.32929 | 0.0000 | 0.0000 | 0.0000 | 0 | 0 | 0 | 0 | 0 | 16 | |
| 2 | 1 | 10 | 200 | 8.723 | 0.32266 | 0.0629 | 0.0081 | 0.07099 | 0.062892 | 0.07099 | 0.062892 | 0.073028 | 0.073028 | 15 | |
| 3 | 1 | 15 | 300 | 5.8357 | 0.29835 | 0.4967 | 0.0378 | 0.534483 | 0.496694 | 0.534483 | 0.496694 | 0.563275 | 0.563275 | 12 | |
| 4 | 1 | 20 | 400 | 3.835 | 0.270725 | 0.7973 | 0.0715 | 0.868818 | 0.797289 | 0.868818 | 0.797289 | 0.909758 | 0.909758 | 4 | |
| 5 | 2 | 5 | 200 | 8.815 | 0.296174 | 0.0491 | 0.0404 | 0.089517 | 0.04907 | 0.089517 | 0.04907 | 0.074542 | 0.074542 | 14 | |
| 6 | 2 | 10 | 100 | 7.5 | 0.282472 | 0.2466 | 0.0572 | 0.303824 | 0.246642 | 0.303824 | 0.246642 | 0.299475 | 0.299475 | 13 | |
| 7 | 2 | 15 | 400 | 4.5 | 0.264554 | 0.6974 | 0.0791 | 0.776443 | 0.697376 | 0.776443 | 0.697376 | 0.804243 | 0.804243 | 7 | |
| 8 | 2 | 20 | 300 | 3.40625 | 0.262446 | 0.8617 | 0.0816 | 0.943348 | 0.861707 | 0.943348 | 0.861707 | 0.985492 | 0.985492 | 2 | |
| 9 | 3 | 5 | 300 | 5.49054 | 0.240465 | 0.5486 | 0.1085 | 0.657041 | 0.548553 | 0.657041 | 0.548553 | 0.656439 | 0.656439 | 10 | |
| 10 | 3 | 10 | 400 | 4.838 | 0.2355775 | 0.6466 | 0.1145 | 0.761051 | 0.646594 | 0.761051 | 0.646594 | 0.766855 | 0.766855 | 9 | |
| 11 | 3 | 15 | 100 | 5.9295 | 0.2336225 | 0.4826 | 0.1168 | 0.599446 | 0.482601 | 0.599446 | 0.482601 | 0.58853 | 0.58853 | 11 | |
| 12 | 3 | 20 | 200 | 4.543 | 0.240465 | 0.6909 | 0.1085 | 0.799404 | 0.690916 | 0.799404 | 0.690916 | 0.812311 | 0.812311 | 6 | |
| 13 | 4 | 5 | 400 | 4.6644 | 0.2292705 | 0.6727 | 0.1222 | 0.794836 | 0.672676 | 0.794836 | 0.672676 | 0.799377 | 0.799377 | 8 | |
| 14 | 4 | 10 | 300 | 3.542 | 0.222666 | 0.8413 | 0.1302 | 0.971538 | 0.841311 | 0.971538 | 0.841311 | 0.988165 | 0.988165 | 1 | |
| 15 | 4 | 15 | 200 | 4.1446 | 0.2273835 | 0.7508 | 0.1245 | 0.875238 | 0.750773 | 0.875238 | 0.750773 | 0.886071 | 0.886071 | 5 | |
| 16 | 4 | 20 | 100 | 3.92265 | 0.216062 | 0.7841 | 0.1383 | 0.922414 | 0.78412 | 0.922414 | 0.78412 | 0.929699 | 0.929699 | 3 | |

when compared with unreinforced composites. The ANOVA findings revealed that the applied load was the main factor for SWR, whereas for COF, the material had more influence. From the output of the VIKOR methodology, parameters like 6 wt%, load at 20 N, and 225 m sliding distance had the best appraisal score. Worn surface morphological characteristics showed that adding filler boosted wear resistance, matching the results of the experimental investigations. Experiment number 14 had the greatest appraisal score of 0.988, which was nearer 1. The VIKOR score revealed that input parameters like material with 6 wt%, a load of 20 N, and a sliding distance of 225 m yielded better characteristics. Based on the evaluation, the options were sorted according to their appraisal score values as $14 < 8 < 16 < 4 < 15 < 12 < 7 < 2 < 10 < 9 < 11 < 3 < 6 < 5 < 2 < 1$.

Acknowledgements This research budget was allocated by the National Science, Research and Innovation Fund (NSRF) (Fundamental Fund 2024) and King Mongkut's University of Technology North Bangkok (Project no. KMUTNB-FF-67-A-03).

References

- Albert FA, Jafrey DJD, Pandiyan GK et al (2022) Tribological studies and optimization of two-body abrasive wear of NaOH-treated *Vachellia farnesiana* fiber by additive ratio assessment method. *J Mater Eng Perform* 32(1):82–90. <https://doi.org/10.1007/s11665-022-07082-y>
- Bahadur S (2000) The development of transfer layers and their role in polymer tribology. *Wear* 245(1–2):92–99. [https://doi.org/10.1016/S0043-1648\(00\)00469-5](https://doi.org/10.1016/S0043-1648(00)00469-5)
- Bhagyashakar MS, Rao RMVGK (2007) Effects of material and test parameters on the wear behavior of particulate filled composites part 1: SiC-epoxy and Gr-epoxy composites. *J Reinf Plast Compos* 26:1753–1768. <https://doi.org/10.1177/07316844070795235>
- Bhuyan RK, Routara BC (2016) Optimization the machining parameters by using VIKOR and entropy weight method during EDM process of Al–18% SiCp metal matrix composite. *Decis Sci Lett* 5(2):269–282
- Birniwa AH, Abdullahi SS, Mahmud HNME (2019) Study on physico-mechanical behaviour of *Acacia nilotica* (Gum Tree) and glass fiber blend reinforced epoxy resin. *Chem Search J* 10(2):46–53. <https://doi.org/10.1177/0021998319860907>
- Durand JM, Vardavoulias M, Jeandin M (1995) Role of reinforcing ceramic particles in the wear behaviour of polymer-based model composites. *Wear* 181–183:833–839. [https://doi.org/10.1016/0043-1648\(95\)90203-1](https://doi.org/10.1016/0043-1648(95)90203-1)
- Formisano A, Boccarusso L, Minutolo FC, et al (2016) Wear behaviour of epoxy resin filled with hard powders. In: AIP Conference Proceedings 1769(1). <https://doi.org/10.1063/1.4963409/934690>
- Fuse K, Dalsaniya A, Modi D et al (2021) Integration of fuzzy AHP and fuzzy TOPSIS methods for wire electric discharge machining of titanium (Ti6Al4V) alloy using RSM. *Materials* 14(23):7408. <https://doi.org/10.3390/ma14237408>
- Jafrey DD, Panneerselvam K (2017) Study on tensile strength, impact strength and analytical model for heat generation in friction vibration joining of polymeric nanocomposite joints. *Polym Eng Sci* 57(5):495–504. <https://doi.org/10.1002/pen.24443>
- Jafrey DD, Panneerselvam K (2020) Experimental investigation and optimization of abrasive wear characteristics of polypropylene nanocomposites. *Mater Res Express* 7:015339. <https://doi.org/10.1088/2053-1591/ab6b52>
- Jankovic A, Chaudhary G, Goia F (2021) Designing the design of experiments (DOE) – an investigation on the influence of different factorial designs on the characterization of complex systems. *Energy Build* 250:111298. <https://doi.org/10.1016/j.enbuild.2021.111298>
- Joseph EJ, Panneerselvam K (2021) Effect of particulate fillers on mechanical, metallurgical and abrasive behavior of tungsten reinforced HDPE composites: a Taguchi approach. *Mater Today Proc* 39:1228–1234. <https://doi.org/10.1016/j.matpr.2020.04.042>
- Kumar R, Kumar R, Soni G et al (2013) Optimization of process parameters during CNC turning by using AHP & VIKOR method. *Int J Eng Res Technol* 2(12):3748–3480. <https://doi.org/10.17577/IJERTV2IS121310>
- Kumar GS, Ramesh M, Dinesh S et al (2022) Investigation of the TIG welding process for joining AA6082 alloy using grey relational analysis. *Adv Mater Sci Eng.* <https://doi.org/10.1155/2022/5670172>
- Kumar SS, Vignesh V, Prasad VVSH et al (2023) Static and dynamic mechanical analysis of hybrid natural fibre composites for engineering applications. *Biomass Convers Biorefinery.* <https://doi.org/10.1007/s13399-022-03689-2>
- Madhu P, Sanjay MR, Sentharamaikannan P et al (2020) Effect of various chemical treatments of *Prosopis juliflora* fibers as composite reinforcement: physicochemical, thermal, mechanical, and morphological properties. *J Nat Fibers* 17:833–844. <https://doi.org/10.1080/15440478.2018.1534191>
- Nirmal U, Yousif BF, Rilling D et al (2010) Effect of betelnut fibres treatment and contact conditions on adhesive wear and frictional performance of polyester composites. *Wear* 268:1354–1370. <https://doi.org/10.1016/j.wear.2010.02.004>
- Pandiyan GK, Prabakaran T, James DJD et al (2021) Improvement on the machinability characteristics of AA6061-T6/15 wt% SiC composites by response surface methodology. *Surf Topogr Metrol Prop* 9(3):035050. <https://doi.org/10.1088/2051-672X/ac2560>
- Pandiyan GK, Prabakaran T, James DJD et al (2022) Machinability analysis and optimization of electrical discharge machining in AA6061-T6/15wt% SiC composite by the multi-criteria decision-making approach. *J Mater Eng Perform* 31(5):3741–3752. <https://doi.org/10.1007/s11665-021-06511-8>
- Raghunath S, Shankar AN, Meena K et al (2021) Multiobjective optimization of mechanical properties on sisal-glass fiber-reinforced hybrid composites using response surface methodology and LINGO analysis. *Adv Mater Sci Eng.* <https://doi.org/10.1155/2021/2376148>
- Raghunathan V, Dhilip JDJ, Subramanian G et al (2021) Influence of chemical treatment on the physico-mechanical characteristics of natural fibers extracted from the barks of *Vachellia farnesiana*. *J Nat Fibers* 19(32):5065–5075. <https://doi.org/10.1080/15440478.2021.1875353>
- Raghunathan V, Palani K, Shinu P et al (2022) Influence of *Parthenium hysterophorus* and *Impomea pes-caprae* fibers stacking sequence on the performance characteristics of epoxy composites. *J Nat Fibers* 19(12):4456–4466. <https://doi.org/10.1080/15440478.2020.1863292>
- Ramesh M, James DJD, Sathish Kumar G et al (2022) Synthesis and characterization of banana and pineapple reinforced hybrid polymer composite for reducing environmental pollution. *Bioinorg Chem Appl* 2022:6344179. <https://doi.org/10.1155/2022/6344179>
- Reddy RVS, Mohana Krishnudu D, Rajendra Prasad P et al (2020) Alkali treatment influence on characterization of *Setaria italic* (Foxtail Millet) fiber reinforced polymer composites using

- vacuum bagging. *J Nat Fibers* 19(5):1851–1863. <https://doi.org/10.1080/15440478.2020.1788494>
- Salisu A, Aujara KM, Yakasai MY (2016) Effect of interface modification on the water absorption and mechanical properties of *Acacia nilotica* fiber-epoxy resin composites. *Int J Adv Sci Eng Technol* 4(1):70–74
- Shi G, Zhang MQ, Rong MZ et al (2004) Sliding wear behavior of epoxy containing nano- Al_2O_3 particles with different pretreatments. *Wear* 256(11–12):1072–1081. [https://doi.org/10.1016/S0043-1648\(03\)00533-7](https://doi.org/10.1016/S0043-1648(03)00533-7)
- Singh MK, Shakyawar DB, Bajpai P et al (2023) Pashmina fiber blended woven fabrics for high functional performances. *J Nat Fibers* 20(1):2139324. <https://doi.org/10.1080/15440478.2022.2139324>
- Sudheer M, Prabhu R, Raju K et al (2014) Effect of filler content on the performance of epoxy/PTW composites. *Adv Mater Sci Eng* 970468:1–11. <https://doi.org/10.1155/2014/970468>
- Vijay R, James DJD, Gowtham S et al (2022) Characterization of natural cellulose fiber from the barks of *Vachellia farnesiana*. *J Nat Fibers* 19(4):1343–1352. <https://doi.org/10.1080/15440478.2020.1764457>
- Vikram KA, Kanth TVK, Prasad RDV et al (2020) Response optimization using VIKOR while machining on lathe under dry and minimum quantity and lubrication conditions – a case study. *Mater Today Proc* 27:2487–2491
- Vinod A, Sanjay MR, Siengchin S (2023) Recently explored natural cellulosic plant fibers 2018–2022: a potential raw material resource for lightweight composites. *Ind Crops Prod* 192:116099. <https://doi.org/10.1016/j.indcrop.2022.116099>
- Xing XS, Li RKY (2004) Wear behavior of epoxy matrix composites filled with uniform sized sub-micron spherical silica particles. *Wear* 256(1–2):21–26. [https://doi.org/10.1016/S0043-1648\(03\)00220-5](https://doi.org/10.1016/S0043-1648(03)00220-5)
- Yahiya M, Venu KN (2022) A review on natural fiber composite with banana as reinforcement. *Mater Today Proc*. <https://doi.org/10.1016/J.MATPR.2023.03.211>

Publisher's Note Springer Nature remains neutral with regard to jurisdictional claims in published maps and institutional affiliations.

Springer Nature or its licensor (e.g. a society or other partner) holds exclusive rights to this article under a publishing agreement with the author(s) or other rightsholder(s); author self-archiving of the accepted manuscript version of this article is solely governed by the terms of such publishing agreement and applicable law.